ARCHIVES OF ELECTRICAL ENGINEERING VOL. 67(2), pp. 321–332 (2018)

DOI 10.24425/119643

Fault Current Limiter optimal sizing considering different Microgrid operational modes using Bat and Cuckoo Search Algorithm

ALI ASGHAR KHODADOOST ARANI[1,2], N. BAYATI[1], REZA MOHAMMADI[1], G.B. GHAREHPETIAN[1], S.H. SADEGHI[1]

[1] *Amirkabir University of Technology*

[2] *Esfahan Electrical Power Distribution Company*
e-mail: asghar.arani@gmail.com

(Received: 07.07.2017, revised: 01.03.2018)

Abstract: Nowadays, the development of smart grids has been the focus of attention due to its advantages for power systems. One of the aspects of smart grids defined by using distributed generation (DG) in a low voltage network is a microgrid (MG). Based on its operational states, MG can operate in different configurations such as grid-connected mode or off-grid mode. The switching between these states is one of the challenging issues in this technical area. The fault currents in different buses have higher value compared to islanded mode of MG when the MG is connected to the main grid, which influences the protection equipment. In this situation, some electrical devices may be damaged due to the fault currents. Application of a fault current limiter (FCL) is considered as an effective way to overcome this challenge. The optimal size of these FCLs can optimize the performance of an MG. In this paper, an index for FCL size optimization has been used. In addition, two optimization algorithms (Bat Algorithm and Cuckoo Search Algorithm) have been applied to the problem. The application of an FCL has been studied in grid-connected and islanded-mode. In addition, the application of the capacitor bank in both modes has been investigated. The results of simulations carried out by MATLAB have been presented and compared.

Key words: fault current limiter (FCL), Bat Algorithm (BA), Cuckoo Search Algorithm (CSA), microgrid (MG)

1. Introduction

Nowadays, the development of advanced technologies and the advent of new requirements such as reducing CO_2 emission in power systems have propelled the conventional power systems to a new power system. The power systems should become smarter to overcome many

challenges. Smart grids equipped by communication technology are new paradigms that have been proposed to solve some problems. Employment of this concept leads to reduction of power loss and increases efficiency and flexibility in power systems [1–4].

Along with smart grids, the application of distributed generations in power distribution networks has created microgrids (MGs). A mart MG consists of some Distributed Generations (DGs), energy storage systems and loads controlled by a Central Controller (CC). The CC can exchange telecommunication signals with all units. The MG can operate either in grid connected or islanded mode [5–6].

Although the DG integration in the MG has some advantages for consumers and power system operators, some problems have emerged by MG development. One of the main problems is the change in protection coordination due to the presence of DGs. As a result, protection devices settings that are coordinated without considering DGs should be altered [7].

Another protection problem occurs when the MG is disconnected from the main grid. The disconnection of the MG from the main grid causes different configurations for the MG. If the MG is connected to the main grid, the fault currents level in MG buses will be more than islanded mode. Due to this difference, protection coordination should be changed by operational mode switching in the MG. Fig. 1 shows the typical MG that can operate in two probable operation modes [8].

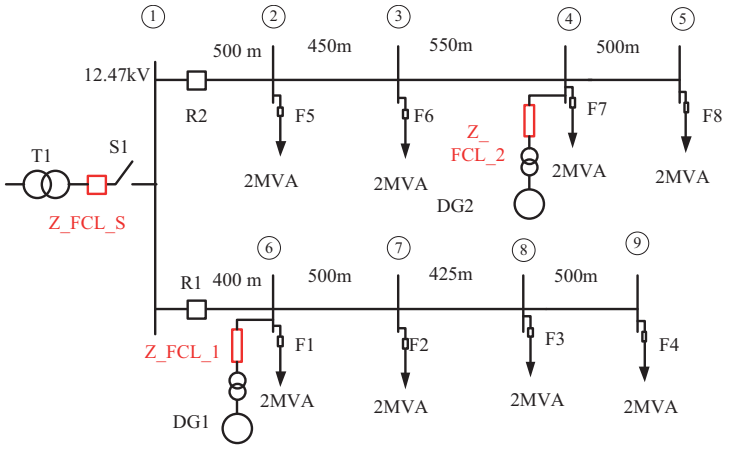

Fig. 1. Typical MG consists of DGs and FCLs [8]

When the applied DGs in the grid are synchronous machines, the fault current in islanded MG does not vary from islanded mode and thus the traditional protection devices can be used. On the other hand, inverter-based DGs that limit their contribution to the fault current cause protection failure [9–12]. To solve this problem, different protection schemes such as digital, admittance and impedance relays have been proposed for this situation [9, 11].

In recent decades, due to power electronics and semiconductor advancement, new solutions for power system problems have been presented. A fault current limiter (FCL) is a power electronic-based device, which limits the fault current when a disturbance such as a fault has

occurred. FCLs can be categorized in two main types: a passive and active type. The passive type is permanently placed in a grid while another type is located in circuit only in fault conditions. The passive type causes excessive losses due to permanent operations. Fig. 2 shows the active FCL structure.

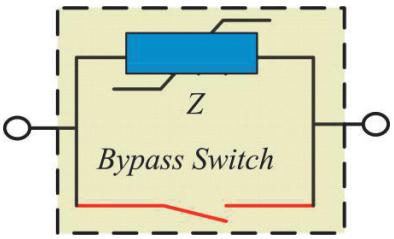

Fig. 2. The active FCL structure

The active FCL has no effect on the normal condition of an MG, power system and fault condition. It has been recognized less than one cycle by the system controller and the limiter impedance (inductance, resistance or capacitance) is activated in the circuit. Fast response and no effect on normal operation of the grid are the advantages of FCLs.

The location of the FCL is an approach that affects the fault current in the grid, and the optimal locating can have a dramatic effect on these currents studied in [13–16]. The genetic algorithm (GA) has been applied to achieve the optimal number and location of the FCL resulting in minimization of the circuit breaker and fuse cost in the grid. Another important issue is the size of FCL impedance. In [16], an FCL has been located in series with DG to avoid protection coordination failure. In both studies, the grid is in grid-connected mode.

As previously mentioned, considering mode changing in the grid, fault currents and consequently protection coordination are failed. An FCL can mitigate the variations in the fault current level. The size of impedance that is selected in fault condition influences the difference between fault currents in operational modes of the MG. In [17] and [18], using particle swarm optimization (PSO) and a GA, respectively, the size of this impedance has been obtained to minimize variations due to MG configuration change.

In this paper, two new and effective optimization algorithms have been used to determine the size of impedance to minimize the variation of fault levels in an MG. As mentioned, the fault currents in an MG are different in various operational modes. The fault currents value in connected mode (to main grid) is high, while in islanded mode it is less. Optimal sizing of FCL placement can decrease the difference of fault currents in different modes. In this paper, the Cuckoo Search Algorithm (CSA) and Bat Algorithm (BA) have been used for optimization. The CSA [19–20] and BA [21–22] have been used for this purpose. In addition to MG mode changing, the application of the capacitor bank has been investigated. The CSA and BA are optimization algorithms inspired from some cuckoo species and some bats, respectively, which have an effective role in different optimization algorithms. In the next section, problem formulation has been carried out. In the third section, two methods have been explained. Simulation results have been presented in section four. Finally, a conclusion has been presented in the last section.

2. Problem description

2.1. Case study

As mentioned, DGs are one of the main elements that have been placed in MGs. Fig. 1 shows the case study of this paper. This MG consists of two feeders and two DGs in these feeders. The MG can be connected or disconnected from the main grid using switch S1.

Since the three phase-balanced fault has a maximum current level in buses, it has been considered for calculations. These currents can be calculated in three configurations of the MG. If the MG is connected to the main grid, the fault currents will increase. In this situation, the DGs can be located in the circuit or not. On the other hand, if the MG is islanded, the fault currents will decrease dramatically. Generally, it can be seen that three probable configurations can be supposed in the MG:

Configuration A. The MG is connected to the main grid but no DGs connected to the MG.

Configuration B. MG is connected to the main grid and two DGs are connected to the MG.

Configuration C. The MG is islanded.

Fig. 3 shows the fault currents of the MG in three configurations. As shown, the difference between fault currents is highly considerable requiring a proper scheme to minimize this difference. A proper solution for this problem, as mentioned, is FCL application. Several FCLs can be located in an MG. These FCLs have been placed in series with two DGs in the main feeders that connect the MG to the main grid (before bus#1).

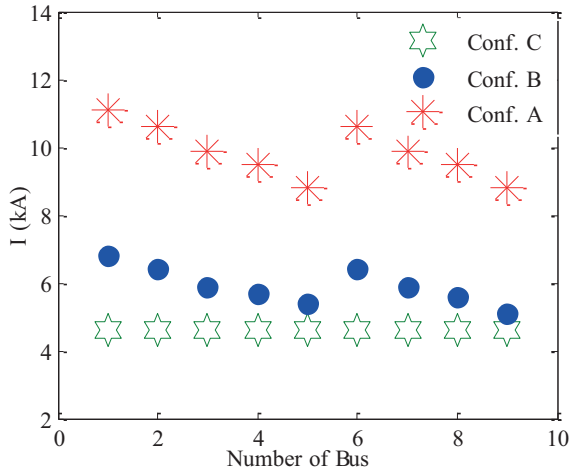

Fig. 3. Fault currents in different configuration of MG

2.2. Problem formulation

To achieve the best size of FCL impedances, the impedance matrix of an MG in three configurations is determined. Based on this, $\boldsymbol{Z}_A$, $\boldsymbol{Z}_B$ and $\boldsymbol{Z}_C$ are the impedance matrices of configurations A, B and C, respectively. To obtain these matrices, firstly admittance matrices ($\boldsymbol{Y}_{\text{bus}-A}$,

$\boldsymbol{Y}_{\text{bus}-B}$ and $\boldsymbol{Y}_{\text{bus}-C}$) are achieved and then inverted. The objective function can be expressed as follows:

$$\text{objective function} = \sum_{i=1}^{m}\sum_{j=1}^{m}(abs(\boldsymbol{Z}_{B_{i,j}} - \boldsymbol{Z}_{A_{i,j}}) + (abs(\boldsymbol{Z}_{C_{i,j}} - \boldsymbol{Z}_{A_{i,j}})), \tag{1}$$

where: parameter m is the number of buses and $\boldsymbol{Z}_A$, $\boldsymbol{Z}_B$ and $\boldsymbol{Z}_C$ represent the elements of impedance matrices in three configurations. In (1), $\boldsymbol{Z}_{A_{i,j}}$ is the impedance matrix of configuration A, which is the base configuration, and two other configurations using FCLs are compared to this configuration. Impedance of FCLs can be expressed as follows:

$$\boldsymbol{Z}_{FCL-s} = R_s + jX_s\,, \tag{2}$$

$$\boldsymbol{Z}_{FCL-1} = R_1 + jX_1\,, \tag{3}$$

$$\boldsymbol{Z}_{FCL-2} = R_2 + jX_2 \tag{4}$$

and the constraints that are applied to impedances are as follows:

$$0 \le R_s \le R_{s-\max}\,, \tag{5}$$

$$0 \le R_{1,2} \le R_{s-\max}\,, \tag{6}$$

$$X_{s-\min} \le X_s \le X_{s-\max}\,, \tag{7}$$

$$X_{\min} \le X_s \le X_{\max}\,. \tag{8}$$

To obtain the best size of FCL impedance, Equation (1) should be minimized. Therefore, a nonlinear equation should be solved which requires the use of heuristic or evolutionary algorithms. In this paper, BA and CSA have been applied to the objective function. In the next sections, two methods have been described and simulated.

3. Optimization algorithms

3.1. Cuckoo Search Algorithm (CSA)

The Cuckoo Search Algorithm was initially developed in 2009 and inspired from a fascinating bird, named cuckoo. Its reproduction was amazing; this bird lays its eggs in the nest of other birds (hosts). These eggs may be recognized by hosts. Among all nests, the best nests that have the best eggs are selected by cuckoo for the next generation. The chicks that hatch from the eggs grow and become a mature cuckoo to create a new society in a new region. The best region will become the purpose of the next generations and, finally, finding the best region is achieved.

Similar to other optimizations, the CSA starts with a population of cuckoos. The cuckoos lay a number of eggs in host birds' nests. Some eggs that are more similar to the hosts' eggs are more probable to survive. A nest that has raised more cuckoo chicks has better quality. The CSA searches for the best nest and region that most eggs can grow in. Fig. 4 shows the flowchart of the CSA and its steps are as follows:

- Step 1. The first population is initialized.
- Step 2. Cuckoos lay the eggs in different host nests.
- Step 3. A fitness function for population evaluation (F_i).
- Step 4. A nest between all nests is chosen (F_j).

– Step 5. Select the best nest between two nests.
– Step 6. The worst nests are abandoned.
– Step 7. Repeat this procedure to satisfy the stop criterion.

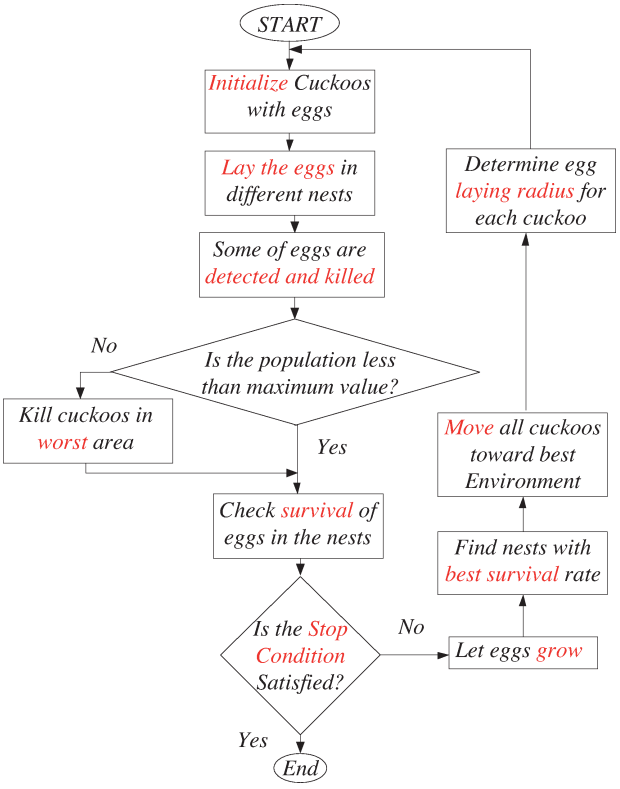

Fig. 4. Cuckoo Search Algorithm flowchart

3.2. Bat Algorithm (BA)

The Bat Algorithm is a new optimization algorithm, which has been inspired from bat behavior for food search. The bats use echolocation by generating ultra sound waves to find their prey location. The waves are reflected from the environment and foods with different levels causing bats to discover their prey. The ability of exchange of waves is an amazing ability that helps the bats hunt, pass obstacles and find their path. Each bat has three basic parameters: location (X_i), velocity (V_i) and quality. The present location of a bat is influenced by its previous location and the best bat location. Each bat changes its route considering the best bat. Based on this bat behavior, the BA can be described as follows:

– Bats use echolocation to determine their routes.
– Bats fly randomly with V_i in X_i with a constant frequency of $f_{\min}$ and different wavelengths of λ and loudness of A_0 to search their preys.
– Bats automatically change the wavelength of their generated waves considering the closeness to the prey by a parameter named pulse release rate (r).
– The sound loudness varies from a minimum value $(A_{\min})$ to a large value (A_0).

Based on the mentioned terms, each bat wants to move to the best bat, and it can be expressed that:

$$X_i^t = X_i^{t-1} + V_i^t, \tag{9}$$

$$V_i^t = V_i^{t-1} + (X_i^t - X^*) f_i, \tag{10}$$

$$f_i^t = f_{\min} + \alpha(f_{\max} - f_{\min}), \tag{11}$$

where: t represents each stage number and α is a random vector between [0, 1] that regulates the frequency in each stage by producing a frequency between maximum $(f_{\max})$ and minimum $(f_{\min})$ frequency.

A bat can receive the best bat signal with probability of *rand*. If it receives this signal, it moves to the best bat. This step can be expressed as follows:

$$\begin{aligned} &if\ (rand) > r_i, \\ &X_{\text{new}} = X_{\text{old}} + \varepsilon^* A^t. \end{aligned} \tag{12}$$

While A is the mean loudness of a bat in the stage of t and ε is a random number between $[-1,\ 1]$. If a bat reaches to its prey, it will produce the minimum loudness $(A_{\min})$ which is assumed to be zero. Considering a bat close to the prey, the generating loudness should be decreased

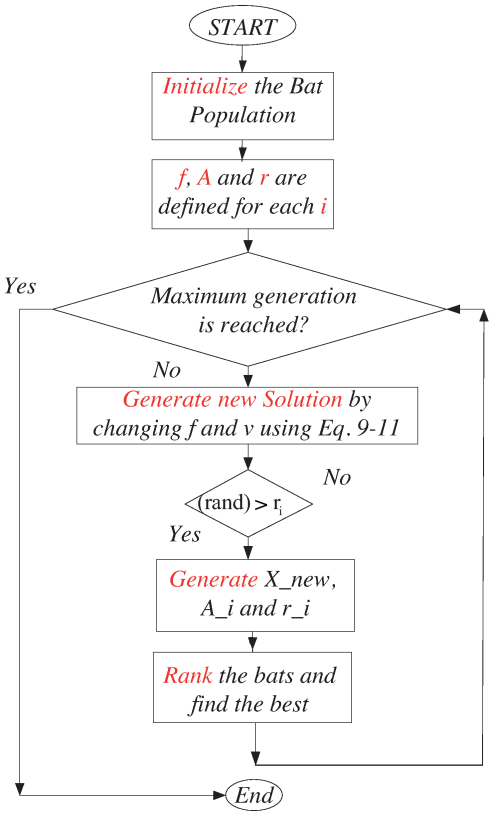

Fig. 5. Bat Algorithm flowchart

as follows:

$$A_i^{t+1} = \beta^* A_i^t, \qquad r_i^{t+1} + r_i^0[1 - \exp(-\gamma t)], \tag{13}$$

where: β is between [0, 1] and γ is a positive value. If the steps tend to a large number, r tends to $r^0$and loudness tends to zero. The flowchart of the BA is shown in Fig. 5.

4. Simulation results

The low voltage network, which has been used for simulation tests, has been shown in Fig. 1. This system consists of two main feeders and two DGs have been applied in this system. Different parameters of the network have been listed in Table 1. As previously mentioned, different short circuit currents of the network, considering DGs and without DGs, have been shown in Fig. 3. The 8 MVA DGs have been installed in bus#2 and 6. The CSA and BA have been used to find the optimal FCL size in an MG.

Table 1. Network and DGs parameters

System characteristics	
Feeder impedance	$Z = 0.1529 + j0.1406$ Ω/km
Network characteristics	$SCC = 500$ MVA and $X/R = 6$
Network transformer parameters	20 MVA, 115/12.47 kv, Dyn, $X^+ = X^- = X^0 = 10\%$, $X_n = 5\%$
Base power and voltage	$S_b = 100$ MVA, $V_b = 12.47$ kV
DG transformer parameters	$X^+ = X^- = X^0 = 5\%$, 12.47 kV/480 V Yn/D
DG reactance	$X^+ = X^- = 9.67\%$, $X^0 = \%$, $X_n = 5\%$

Fig. 6 shows the convergence procedure of two methods. These two methods have been run by 200 iterations and the final values of the objective function and the impedances size have been listed in Table 2. Each algorithm has been run 50 times and the best results have been presented. In this stage, it is assumed that the FCL impedance has resistive and inductive parts or resistive part only (no capacitive part).

Table 2. FCL sizes and objective function values by resistive and inductive FCL

FCL impedance	**Resistive and inductive**		**Resistive only**	
	BA	CSA	BA	CSA
Z_1_TCI	$0.0001 + 0j$	$0.0897 + j0$	4.0811	4.0811
Z_2_TCI	$0.0003 + 0j$	$0.1047 + j0$	0	0
Z_s_TCI	$1.0109 + j2.2974$	$0.4584 + j2.5584$	0	0
Objective function	17.6087	17.12	31.8761	31.8761

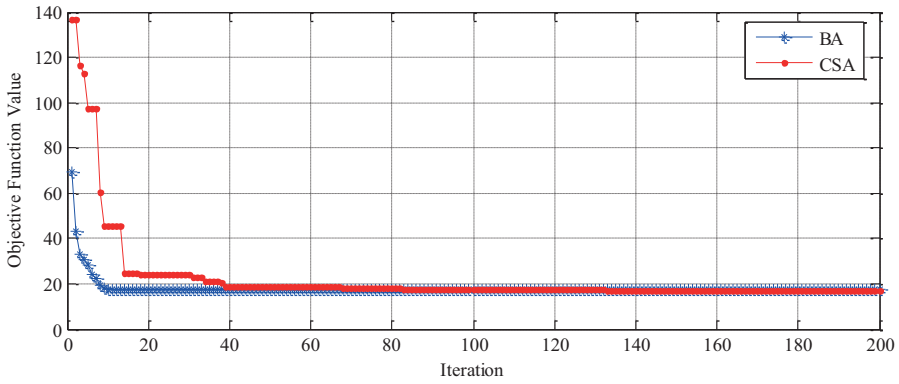

Fig. 6. The convergence process of both algorithms (resistive and inductive cases only)

In addition, two algorithms have been applied for a capacitive and inductive FCL and their results have been presented. Fig. 7 shows the convergence procedure of two methods for these cases. These two methods have been run by 200 iterations and the objective function and the impedances sizes have been listed in Table 3. The results show that the capacitive FCL can minimize the objective function more than inductive or resistive ones, which means that the difference between the short circuit currents is less than the two others.

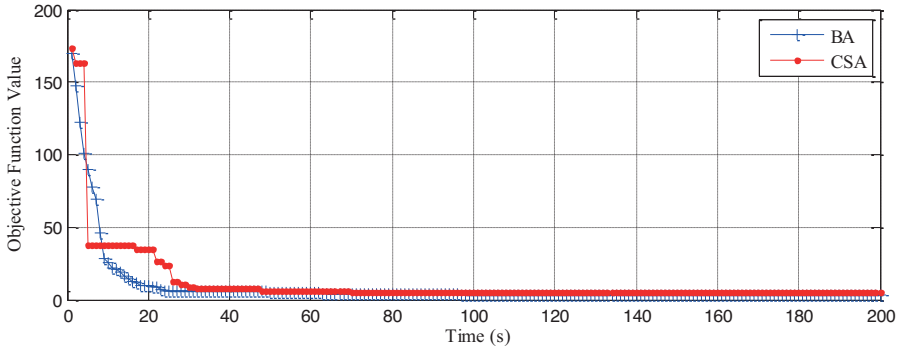

Fig. 7. The convergence process of both algorithms (assuming capacitive and inductive cases)

Fig. 8 shows the fault currents in grid connected mode with and without the FCL. As it can be seen, the fault currents using the FCL have been decreased, which affects the operation of protection equipment. As shown in the illustration, the fault current in bus#6 is decreased from nearly 11 kA to 6 kA. In addition, other fault currents have been reduced which shows the effectiveness of FCL sizing. On the other hand, the difference between fault currents (for two buses) in two scenarios has been decreased dramatically; as shown in Fig. 8 for bus#5 and bus#6.

Another simulation scenario has been carried out by locating the capacitor bank in the MG. Considering the capacitor bank in bus#1, with an impedance equal to $-0.5j$, the FCL sizes have been obtained. The negative imaginary part of this impedance decreases the total impedance

Table 3. FCL sizes and objective function values inductive and capacitive FCL

FCL impedance	Inductive and capacitive		Inductive only	
	BA	CSA	BA	CSA
Z_1_TCI	$0.1171 - j0.2462$	$0 - j0.3586$	2.4626	2.4626
Z_2_TCI	$0.0173 - j0.5933$	$0.1819 - j0.4083$	0	0
Z_s_TCI	$9.9940 - j9.9999$	$10.0 + j10.0$	0	0
Objective function	3.0900	3.5216	21.0076	21.0076

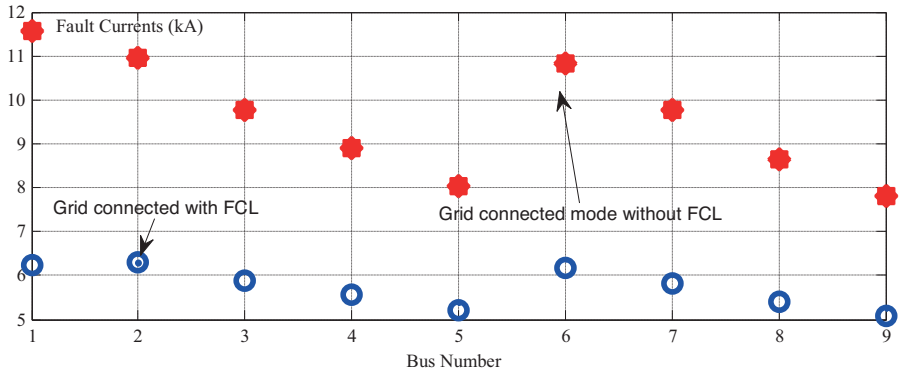

Fig. 8. Fault currents in grid-connected mode with and without FCL

and consequently, the fault currents increase. The results of the BA and CSA have been listed in Table 4. By applying the achieved FCL in the simulation, it can be seen that the differences between the fault currents for all buses in this scenario have been reduced as shown in Fig. 9.

Table 4. FCL sizes and objective function values by assuming capacitor bank in bus#1

FCL impedance	Inductive and capacitive	
	BA	CSA
Z_1_TCI	$10.00 - j10.00$	$10.00 - j9.9999$
Z_2_TCI	$0.0413 - j0.5899$	$0.00 - j0.0613$
Z_s_TCI	$0.1687 - j0.0969$	$0.1324 + j0.6279$
Objective function	3.3873	3.9045

Obviously, the difference between fault currents in two configurations (A and B) without the FCL is high (sometimes more than 2 kA), while these values are less than 0.5 kA with optimal sizing of FCL placement. For configuration of C and A, this decrement is clearly observable considering Fig. 9.

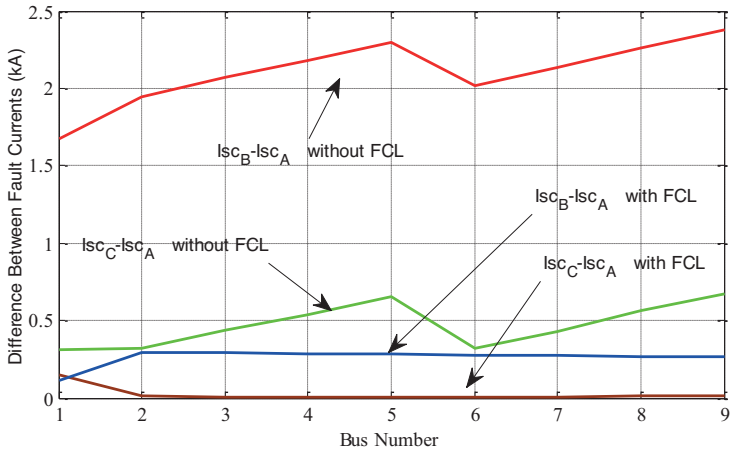

Fig. 9. Fault currents in grid-connected mode with and without FCL

5. Conclusion

In this paper, by using FCLs, an attempt is made to decrease the difference between various operational modes of an MG. The MG consists of two DGs and can operate in grid-connected or islanded mode. To optimize the FCL size, the impedance matrices of three operational modes have been initially computed. An objective function has been defined using these matrices. To optimize the objective function, two optimization algorithms (BA and CSA) have been applied to the problem. The result of optimization algorithms for different FCL types such as (resistive, inductive, and capacitive) has been presented by using two optimization algorithms. In addition, the application of the FCL by using the capacitor bank in the MG has been studied. Application of an optimal size of the FCL decreases the difference between fault currents in different operational modes and consequently decreases coordination failures. The application of optimally sized FCL decreases the difference between fault currents in different configurations (from 5 kA to lower than 0.5 kA).

References

[1] Morandi A., *State of the art of superconducting fault current limiters and their application to the electric power system*, Physica C: Superconductivity, vol. 484, pp. 242–247 (2013).

[2] Walling R.A., Saint R., Dugan R.C., Burke J., Kojovic L.A., *Summary of distributed resources impact on power delivery systems*, IEEE Trans. Power Del., vol. 23, no. 3, pp. 1636–1644 (2008).

[3] Yang G.-Y., Jiang D.-Z., Lu X., Lin R., Wu Z.-L., *Control strategy & test study of SSFCL with bi-directional current*, Power and Energy Society General Meeting – Conversion and Delivery of Electrical Energy in the 21st Century, Pittsburgh, PA, USA, pp. 1–8 (2008)

[4] Arani K.A.A., Gharehpetian G.B., *Enhancement of microgrid frequency control subsequent to islanding process using flywheel energy storage system*, in Smart Grid Conference (SGC), Tehran, Iran, pp. 1–6 (2014)

[5] Kaur A., Kaushal J., Basak P., *A review on microgrid central controller*, Renewable and Sustainable Energy Reviews, vol. 55, pp. 338–45 (2016).

[6] Meng L., Savaghebi M., Andrade F., Vasquez J.C., Guerrero J.M., Graells M., *Microgrid central controller development and hierarchical control implementation in the intelligent microgrid lab of Aalborg University*, In Applied Power Electronics Conference and Exposition (APEC), Charlotte, NC, USA, pp. 2585–2592 (2015).

[7] Basak P., Chowdhury S., Dey S.H., Chowdhury S.P., *A literature review on integration of distributed energy resources in the perspective of control, protection and stability of microgrid*, Renewable and Sustainable Energy Reviews, vol. 16, no. 8, pp. 5545–56 (2012).

[8] Zeineldin H., El-Saadany E.F., Salama M.M., Kasem Alaboudy A.H., Woon W.L., *Optimal Sizing of Thyristor-Controlled Impedance for Smart Grids With Multiple Configurations*, Smart Grid IEEE Transactions on, vol. 2, no. 3, pp. 528–537 (2011).

[9] Sortomme E., Venkata S.S., Mitra J., *Microgrid protection using communication-assisted digital relays*, IEEE Trans. Power Del., vol. 25, no. 4, pp. 2789–2796 (2010).

[10] Nikkhajoei H., Lasseter R.H., *Microgrid protection*, in Proc. IEEE Power Eng. Soc. Gen. Meet., Tampa, FL, USA, pp. 1–6 (2007).

[11] Dewadasa M., Majumder R., Ghosh A., Ledwich G., *Control and protection of a microgrid with converter interfaced micro sources*, in Proc. Int. Conf. Power Syst. (ICPS), Kharagpur, India, pp. 1–6 (2009).

[12] Han Y., Hu X., Zhang D., *Study of adaptive fault current algo rithm for microgrid dominated by inverter based distributed generators*, in Proc. 2nd IEEE Int. Symp. Power Electron. Distrib. Gener. Syst. (PEDG), Hefei, China, pp. 852–854 (2010).

[13] Sortomme E., Venkata S.S., Mitra J., *Microgrid protection using communication-assisted digital relays*, IEEE Trans. Power Del., vol. 25, no. 4, pp. 2789–2796 (2010).

[14] Teng J-H., Lu C-N., *Optimum fault current limiter placement with search space reduction technique*, IET generation, transmission & distribution, vol. 4, no. 4, 485–494 (2010).

[15] Basak M. *et al.*, *A literature review on integration of distributed energy resources in the perspective of control, protection and stability of microgrid*, Renewable and Sustainable Energy Reviews, vol. 16, no. 8, pp. 5545–5556 (2012).

[16] Habib H.F., Tarek Y., Mehmet H.C., Osama A.M., *Multi-Agent-Based Technique for Fault Location, Isolation, and Service Restoration*, IEEE Transactions on Industry Applications, vol. 53, no. 3, pp. 1841–1851 (2017).

[17] Pedrasa M.A.A., Spooner T.D., MacGill I.F., *Coordinated scheduling of residential distributed energy resources to optimize smarthome energy services*, IEEE Trans. Smart Grid, vol. 1, no. 2, pp. 134–143 (2010).

[18] Zeineldin H., El-Saadany E., Salama M., *Optimal coordinationof overcurrent relays using a modified particle swarm optimization*, Elect. Power Syst. Res., vol. 76, no. 11, pp. 988–995 (2006).

[19] Gandomi A.H., Yang X.S., Alavi A.H., *Cuckoo search algorithm: a metaheuristic approach to solve structural optimization problems*, Engineering with computers, vol. 29, no. 1, pp. 17–35 (2013).

[20] Gokhale S.S., Kale V.S., *Time overcurrent relay coordination using the Levy flight Cuckoo search algorithm*, InTENCON 2015-2015 IEEE Region 10 Conference, Macao, China, pp. 1–6 (2015).

[21] Kheirollahi R., Namdari F., *Optimal coordination of overcurrent relays based on modified BAT optimization algorithm*, International Electrical Engineering Journal (IEEJ), vol. 5, no. 2, pp. 1273–1279 (2014).

[22] Yang X.S., Hossein Gandomi A., *Bat algorithm: a novel approach for global engineering optimization*, Engineering Computations, vol. 29, no. 5, pp. 464–483 (2012).